Uptake of SO_2 on HOBr−Ice Surfaces

Ronghua Jin and Liang T. Chu*

Wadsworth Center, New York State Health Department and Department of Environmental Health Sciences, State University of New York at Albany, P.O. Box 509, Albany, New York 12201-0509

Received: November 9, 2005; In Final Form: January 11, 2006

The uptake of SO_2 on HOBr-treated ice surfaces has been studied using a flow reactor coupled with a differentially pumped quadrupole mass spectrometer at 190−240 K. The initial uptake coefficient was determined as a function of HOBr surface coverage, θ_{HOBr}, on the ice. The uptake coefficients increase as the HOBr coverage increases. The uptake coefficient can be expressed as $\gamma_t = k_h\theta_{HOBr}$, where $k_h = 1.5 \times 10^{-19}$ molecules^{-1} cm^{-2} at 191 K and $k_h = 6.4 \times 10^{-21}$ molecules^{-1} cm^{-2} at 210 K and θ_{HOBr} is in the range of 8×10^{13} to 1.2×10^{15} molecules cm^{-2}. The effects of temperature and film thickness on the uptake coefficients of SO_2 by the HOBr-treated ice films were also studied. The activation energy E_a of SO_2 on HOBr−ice surfaces is approximately -81 ± 8 kJ/mol in the 190−215 K range. Kinetic results were interpreted in terms of the Eley−Rideal mechanism. This study suggests that the uptake of SO_2 on ice/snow surfaces is enhanced by the presence of HOBr near the ice surface. The implication for atmospheric chemistry is that HOBr−ice surfaces may not provide a significant pathway to oxide S(IV) in the boundary layer due to both lower uptake coefficient and smaller HOBr surface coverage at $T > 220$ K.

I. Introduction

It has been discovered in recent years that the Arctic atmosphere is highly polluted during winter, because of strong transport from Eurasia to the pole and weak pollutant removal by precipitation at cold temperatures.[1] The pollution level has been increasing since the 1950s due to increasing industrial activity.[2] Recently, considerable attention has been focused on the role of chemistry in the marine boundary layer (MBL), which cycles ozone, bromine, chlorine, and sulfur oxides.[3−5] Barrie et al. have suggested that ozone is destroyed in the MBL during polar sunrise, by a mechanism involving Br and BrO.[6,7] Fan and Jacob proposed a bromine cycle mechanism.[8] Chlorine and bromine in the MBL can affect the concentrations of ozone, hydrocarbons, and cloud condensation nuclei.

Sulfur dioxide is one of the key pollutants in the atmosphere. When it is released into the atmosphere, SO_2 undergoes oxidation processes and eventually is converted to sulfate in the form of acid rain and snow, which reach the ground as precipitates. The oxidation of S(IV) in the atmosphere is of great interest, due to the toxicity and deleterious environmental effects of sulfate. Field measurements have shown that the concentration of sulfate in freshly fallen snow is higher than would be expected from particulate sulfate scavenging.[9,10] This result is pertinent to the question of how gaseous SO_2 enters snow ice, by uptake.

A model study has suggested that nearly 40% of S(IV) scavenged by sea-salt aerosols is oxidized by HOCl, and ∼20% by HOBr, in the remote MBL.[11] The remaining S(IV) is oxidized by ozone, H_2O_2, and other oxidants. It is uncertain how rapidly HOBr molecules can oxide SO_2 on snow ice particle surfaces. Also unclear is the impact on the HOBr/bromine activation near snow/ice surfaces due to SO_2 oxidation by HOX.

The SO_2 concentration is 50 pptv in the free troposphere, and the mean SO_2 concentration over the Atlantic is $0.24^{+0.98}_{-0.24}$ ppbv.[12,13] SO_2 can be taken up by snow ice and sea-salt aerosol, and adsorbed SO_2 is oxidized readily.[12−15] Several groups have studied the incorporation of SO_2 in ice.[16−19] These studies showed that the concentration of SO_2 in water-ice reaches a maximum in a temperature range of 0 to −10 °C, due to the presence of a quasi-liquid layer near the ice surface.[20,21] The interaction of SO_2 with both water-ice and H_2O_2-treated ice surfaces has been investigated recently.[22,23] The oxidation of SO_2 was shown to be accelerated by the presence of small amounts of H_2O_2 (0.8−3 wt %) in ice.[22]

Halogen compounds have a significant impact on the chemistry of the boundary layer. The boundary-layer ozone loss in the polar springtime is a good example. HOBr is a major bromine-containing compound in the MBL. HOBr has been shown to oxidize S(IV) rapidly in solution,[24,25] and atmospheric chemistry modeling calculations suggested that S(IV) oxidation by HOBr and HOCl in deliquescent sea-salt ice particles in the pH range of 5.5−7 is an important process in the MBL.[11,26] The modeling calculation, which was based on the aqueous-phase rate constants, suggested that the pathway accounts for the oxidation of up to 60% of S(IV) in the boundary layer by HOCl and HOBr. Deliquescent sea-salt particles contain mainly Cl^- and Br^-, and HOBr molecules scavenged from the particles can react with these halide ions. Like in aqueous-phase chemistry, S(IV) oxidation is presumably determined by HOBr and HOCl near the particle surfaces. Water-ice and sea-salt ice are important particulates in the MBL, and atmospheric concentrations of SO_2 (0.24 ppbv)[12] and HOBr (0.26 ppbv)[27] are comparable. It is most suitable to investigate the SO_2 reactive uptake on HOBr-treated ice surfaces to test this hypothesis. To the best of our knowledge, no direct measurement of the SO_2 oxidation with HOBr on water-ice surfaces has been reported in the literature. This motivated us to study the heterogeneous uptake of SO_2 with HOBr on ice surfaces at low temperatures and to assess the importance of S(IV) oxidation in the boundary layer.

In this paper, we report the first measurement of the uptake coefficient of SO_2 on HOBr-treated ice surfaces at 190−240

* To whom correspondence should be addressed. E-mail: lchu@albany.edu.

10.1021/jp0564952 CCC: $33.50
Published on Web 02/10/2006

K. In the following sections, we will briefly describe the experimental procedures used in the determination of the uptake coefficient. We will consider the initial uptake coefficient for SO_2 on HOBr-treated ice surfaces as a function of HOBr surface coverage (uptake amount) and ice-film temperature and thickness. The results will be discussed in terms of a reaction mechanism.

II. Experimental Section

The measurements of the uptake coefficient of SO_2 on the HOBr-treated ice surface were performed in a flow reactor coupled to a differentially pumped quadrupole mass spectrometer (QMS). The flow-tube reactor and QMS vacuum system were interfaced by means of a flexible stainless steel bellows and were separated by a valve. The details of the apparatus have been given in our previous publications;[28−30] here, we will provide a brief description that includes some modifications made for the present study.

2.1. Flow Reactor. The cylindrical flow reactor was made of Pyrex glass with an inner diameter of 1.70 cm and a length of 35 cm. The outer jacket was a vacuum layer, to maintain the temperature of the reactor. The temperature of the reactor was regulated by a liquid nitrogen cooled methanol circulator (Neslab) and was measured with a pair of J-type thermocouples located in the middle and at the downstream end of the reactor. During the experiment, the temperature was maintained at 190−240 K; the stability of the temperature was better than ±0.3 K for every measurement. The total pressure of the flow reactor was controlled by a downstream throttle valve (MKS Instrument, Model 651C) and was measured with a high-precision Baratron pressure gauge (MKS Instrument, 690A). The stability of the pressure was better than ±0.001 Torr. A double-capillary Pyrex injector was used to introduce HOBr, He−water vapor, and SO_2 into the system. To avoid water vapor condensation on the capillary at low temperatures, room-temperature dry air was passed through the outside of the capillary to keep it warm.

2.2. Ice-film Preparation. The ice film was prepared by passing helium carrier gas (BOC, 99.9999%) through a high-purity distilled water (Millipore Milli-Q plus, >18 MΩ cm) reservoir. The reservoir was maintained at 293.2 ± 0.1 K by a refrigerated circulator (Neslab, RTE-100LP). Helium saturated with the water vapor was admitted to an inlet of the double-capillary injector. During the course of the ice deposition, the double-capillary injector was slowly pulled out at a constant speed and a uniform ice film was deposited on the inner surface of the reactor, which was at a temperature of the experiment. The amount of ice−substrate deposited was determined from the water vapor pressure, the mass flow rate of the helium−water mixture, which was measured by a Hasting mass flow meter, and the deposition time. The average film thickness, h, was calculated from the mass of ice, the geometric area of the film on the flow reactor, and the bulk density ($\rho_b = 0.63$ g/cm^3) of vapor-deposited water-ice.[31] For the uptake coefficient of SO_2 on HOBr-treated ice surface measurements, the typical average film thickness was about 3.0 μm at 190 K and 7.6 μm at 210 K. The ice-film sublimation rate is higher at warmer temperature,[32] which increases the dynamic nature of the ice-film surface. Under the constant flow conditions, the ice vapor was carried away and the loss was approximately 2.7×10^{-3} mg/h at 191 K with a total ice-film mass of 10−500 mg. Along with the higher total pressure in the reactor, we prepared a thicker ice film on the wall of the flow reactor and an additional section of ice was deposited in the upstream end to compensate for the migration of ice from the upstream to downstream end in each experiment. By doing so, the ice-film loss was minimized at higher temperatures.

2.3. HOBr Preparation and Calibration. The HOBr solution was prepared by the addition of bromine (Aldrich, 99.5%) in successive portions to an ice-cooled glass flask,[33,34] in which 2.1 g of $AgNO_3$ (Baker, 99.9%) had been dissolved in 100 mL of distilled H_2O, until the orange color indicative of excess bromine persisted under continued stirring. The solution was then filtered to remove all precipitated AgBr. The filtered solution was freed of Br_2 by five successive extractions with CCl_4. A slightly yellowish clear HOBr solution was obtained and was kept in a bubbler at 273.2 K in the dark.[35]

The HOBr vapor was bubbled into the movable injector by helium gas, through the PFA tubing connected by Teflon Swagelok. The flow rate was controlled by a Monel metering valve, which was treated with Halocarbon grease. The concentration of HOBr vapor was calibrated by reacting it with HCl on ice surfaces at 190 K, in a separate experiment.[35] In the HOBr calibration experiment, a higher concentration of HOBr was admitted into the flow reactor and the entire ice surface was exposed to HOBr for more than 10 min, so as to achieve sufficient surface coverage. Then, HCl was introduced into the flow reactor, and it was reacted with adsorbed HOBr molecules to produce BrCl. Since the HCl concentration was precisely prepared, HOBr was in excess, and assuming that the reaction followed the 1:1 stoichiometric ratio, the loss of one HCl molecule was equal to the formation of one BrCl molecule. Thus, we have determined the signal ratio of HCl to BrCl by the QMS. In another experiment, HCl was in excess and the same experimental procedures were repeated. In this case, the loss of HOBr molecules was equal to the formation of BrCl molecules. We measured the signal ratio of HOBr to BrCl. From these two experiments, we determined the signal ratio (QMS counts) of HOBr to HCl. These measurements were conducted at various QMS multiplier voltages. The ratio was approximately constant at slightly differing QMS multiplier voltages, provided that the ionization voltage and emission current were constant. Knowing both the signal ratio of HOBr to HCl and the HCl concentration, we have determined the gas-phase HOBr concentration.

2.4. SO_2−He Mixtures. The SO_2−He mixture was prepared by mixing SO_2 (Linde, 99.98%) and helium in an all-glass manifold, which had been previously evacuated to $\sim 10^{-6}$ Torr. SO_2 was a high-purity commercial gas and was not further purified. The typical SO_2-to-He mixing ratio was $\sim 10^{-5}$. SO_2, along with additional helium carrier gas, controlled by metering valves, was introduced into the flow reactor via the glass and PFA tubing. All of the tubing was passivated by the SO_2−He mixture so as to establish equilibrium, as monitored by the QMS prior to every experiment. The amount of the SO_2 and helium mixture was controlled by two stainless steel metering valves in series, and the flow rate was determined from the pressure change in the manifold per minute. The typical pressure in the manifold was ∼400 Torr, and the volume of the manifold was large (12 L). The change of pressure in the manifold was several Torr for the duration of the experiment. Therefore, the SO_2 flow rate was constant during the experiment.

2.5. Determination of the Uptake Coefficient. The uptake coefficient γ_w for SO_2 on the HOBr-treated ice film was determined as follows. First, a fresh ice film was prepared by water vapor deposition on the inner wall of the flow reactor, as described in section 2.2, for every measurement. Second, the helium carrier gas was bubbled through the HOBr solution, which was kept at 273.15 K. The HOBr vapor−He mixture

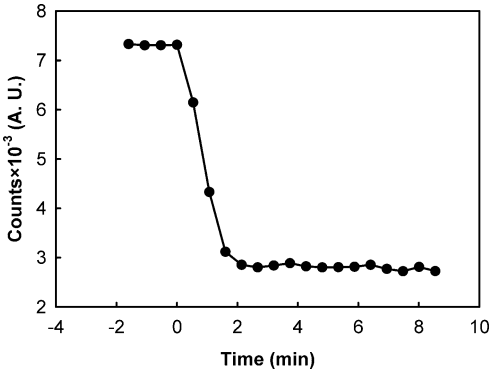

Figure 1. Plot of HOBr signal vs exposure time, for HOBr uptake by water-ice, at $P_{HOBr} = 1.4 \times 10^{-6}$ Torr and 190.8 K. (●) represents the HOBr signal. The plot shows the initial signal, before HOBr came in contact with water-ice ($t < 0$); the uptake, starting at $t = 0$ min when HOBr was exposed to the ice film; and the loss of HOBr on the ice film. The HOBr background signal was corrected. The HOBr coverage is 4.5×10^{14} molecules/cm^2. The total pressure is 0.500 ± 0.001 Torr, the flow velocity is 14.9 m/s, and the ice-film thickness is 3.0 μm.

was then admitted to an inlet of the double-capillary injector. Before exposure of HOBr to the ice film, an initial HOBr signal was determined by the QMS. The sliding injector was then slowly pulled out (∼2 cm/min) toward the upstream end of the flow reactor to uniformly expose HOBr onto the ice surface. Gas-phase HOBr was taken up by the freshly prepared ice surface. The loss of HOBr was monitored by the QMS at $m/e^- = 96$. The data acquisition time was typically 10−30 s/point. Since the HOBr exposure time was well-controlled, the amount of HOBr on the ice surface, that is, the coverage, was also well-controlled. The uptake amount of HOBr was determined by integration of the calibrated HOBr signal over the exposure time. A typical HOBr uptake amount on the water-ice film at 191 K is shown in Figure 1. The sliding injector was pushed back to the downstream end to prepare for the SO_2 uptake coefficient measurement. Finally, SO_2, at a partial pressure ranging between 9.5×10^{-7} and 1.6×10^{-6} Torr, was exposed to the HOBr-treated ice-film surface. The injector was pulled toward the upstream end 2 cm at a time, and the injector position was recorded. The gas-phase loss of SO_2 was measured by the QMS at $m/e^- = 64$ as a function of the injector distance z. For the pseudo-first-order rate under plug-flow conditions, the following equation holds for SO_2

$$\ln[SO_2]_z = -k_s(z/\upsilon) + \ln[SO_2]_0 \qquad (1)$$

where z is the injector position, υ is the flow velocity, $[SO_2]_z$ is the gas-phase SO_2 concentration measured by the QMS at position z, and subscript 0 is the initial injector reference position. The first-order SO_2 decay for a typical experiment performed on the HOBr-treated ice film at 191 K is shown in Figure 2. The first-order loss rate constant, k_s, was calculated from the least-squares fit of the experimental data to eq 1. $k_s =$ 13.4/s at 191 K, as shown in Figure 2. k_s was corrected for gas-phase axial and radial diffusion using a standard procedure,[36] and the corrected rate constant is termed k_w. A diffusion coefficient (cm^2/s) for SO_2 in helium was used for the gas-phase diffusion correction; it was estimated using the Fuller equation. This can be expressed as[22,37]

$$D = 1.649 \times 10^{-2} T^{1.75}/P \qquad (2)$$

where T is the temperature in Kelvin and P is the total pressure of the reactor in Torr. The uptake coefficient γ_w was calculated

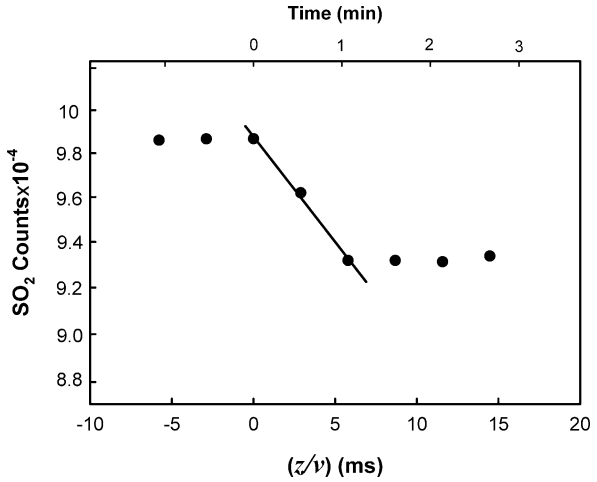

Figure 2. Plot of the log SO_2 signal vs the reaction time (z/υ) on HOBr-treated ice at $P_{SO_2} = 1.5 \times 10^{-6}$ Torr and 190.5 K. The plot shows the initial SO_2 signal, before the SO_2 came in contact with the HOBr-treated ice ($t < 0$) and the loss of SO_2 on the film. The pseudo-first-order rate constant is $k_s = 13.4$ s^{-1}, and the corrected rate constant is $k_w = 13.7$ s^{-1}. The initial uptake coefficient is $\gamma_w = 9.3 \times 10^{-4}$. HOBr coverage is 8.9×10^{14} molecules/cm^2. The partial pressure of P_{HOBr} is 1.4×10^{-6} Torr. The total pressure of the reactor is 1.000 ± 0.002 Torr, and the background SO_2 signal was corrected.

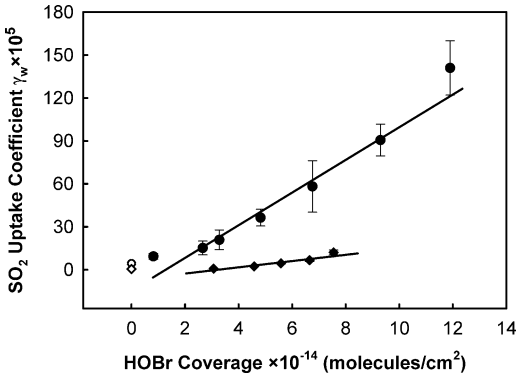

Figure 3. Plot of the initial uptake coefficient of SO_2 γ_w vs the HOBr surface coverage. (●) is γ_w on HOBr-treated ice films at 191 K, and (♦) is at 210 K. The thickness of the ice film is 3.0 ± 0.2 μm at 191 K and 7.6 ± 0.2 μm at 210 K. The partial pressure of SO_2 is $(1.4 \pm 0.2) \times 10^{-6}$ Torr, and the total pressure in the reactor is 1.000 ± 0.002 Torr. The plot indicates that γ_w increases as HOBr coverage increases and that γ_w is higher at 191 K. Error bars represent 1 standard deviation of the mean. Solid lines are drawn as a visual aid. The uptake coefficients for SO_2 on water-ice surfaces are also included; they are denoted by (○) at 191 K and (◊) at 210 K.

from k_w using the following equation[38]

$$\gamma_w = 2Rk_w/(\omega + Rk_w) \qquad (3)$$

where R is the radius of the flow reactor (0.85 cm) and ω is the mean SO_2 molecular velocity at the HOBr-treated ice-film temperature.

The typical amount of SO_2 loss to the HOBr-treated ice surface is on the order of 10^{12} molecules/cm^2; this value was determined by integrating the SO_2 QMS signal over the experimental time (the exposure time is labeled on the top y-axis in Figure 2). It is approximately 100-fold lower than the HOBr coverage (typically 10^{14} molecules/cm^2; see Figure 3). The pseudo-first-order rate approximation (eq 1) treatment is justified. Since the k_s value is small, the number of data points that can be collected is limited as shown in Figure 2. This is the case for most data presented except for some thicker ice-film

TABLE 1: Uptake Coefficients of SO_2 on HOBr-treated Ice Surfaces[a]

temperature (K)	P_{SO_2} (Torr)	v (m/s)	HOBr uptake amount (molecules/cm^2)	k_s (1/s)	k_w (1/s)	γ_w	γ_t[b]
190.8 ± 0.2	1.6×10^{-6}	6.9	0	0.65 ± 0.09	0.65 ± 0.10	$(4.4 \pm 0.6) \times 10^{-5}$	2.0×10^{-6} [c]
190.6 ± 0.4	1.4×10^{-6}	6.8	8.2×10^{13}	1.38 ± 0.31	1.38 ± 0.31	$(9.3 \pm 2.1) \times 10^{-5}$	1.2×10^{-5}
190.5 ± 0.2	1.5×10^{-6}	6.8	2.7×10^{14}	2.24 ± 0.71	2.25 ± 0.75	$(1.5 \pm 0.5) \times 10^{-4}$	2.0×10^{-5}
190.8 ± 0.2	1.6×10^{-6}	7.0	3.3×10^{14}	3.07 ± 1.01	3.09 ± 1.02	$(2.1 \pm 0.7) \times 10^{-4}$	2.7×10^{-5}
190.6 ± 0.2	1.4×10^{-6}	6.9	4.8×10^{14}	5.33 ± 0.86	5.37 ± 0.87	$(3.6 \pm 0.6) \times 10^{-4}$	4.7×10^{-5}
190.7 ± 0.7	1.5×10^{-6}	6.9	6.8×10^{14}	8.49 ± 2.61	8.59 ± 2.66	$(5.8 \pm 1.8) \times 10^{-4}$	7.6×10^{-5}
190.5 ± 0.2	1.5×10^{-6}	6.9	9.3×10^{14}	13.2 ± 1.6	13.4 ± 1.6	$(9.1 \pm 1.1) \times 10^{-4}$	1.2×10^{-4}
190.8 ± 0.4	1.4×10^{-6}	6.9	1.2×10^{15}	20.3 ± 2.7	20.9 ± 2.8	$(1.4 \pm 0.2) \times 10^{-3}$	1.8×10^{-4}
210.0 ± 0.1	1.3×10^{-6}	4.5	0	0.07 ± 0.01	0.07 ± 0.01	$(4.7 \pm 0.5) \times 10^{-6}$	1.3×10^{-7}
210.1 ± 0.1	1.3×10^{-6}	4.5	3.1×10^{14}	0.12 ± 0.02	0.12 ± 0.02	$(7.8 \pm 1.2) \times 10^{-6}$	2.1×10^{-7}
210.1 ± 0.2	1.5×10^{-6}	4.5	4.6×10^{14}	0.37 ± 0.05	0.37 ± 0.05	$(2.4 \pm 0.3) \times 10^{-5}$	6.5×10^{-7}
210.2 ± 0.1	1.6×10^{-6}	4.6	5.6×10^{14}	0.70 ± 0.10	0.70 ± 0.09	$(4.5 \pm 0.5) \times 10^{-5}$	1.2×10^{-6}
210.2 ± 0.2	1.4×10^{-6}	4.5	6.7×10^{14}	1.04 ± 0.14	1.04 ± 0.14	$(6.7 \pm 0.9) \times 10^{-5}$	1.8×10^{-6}
210.1 ± 0.2	1.5×10^{-6}	4.5	7.6×10^{14}	1.88 ± 0.26	1.89 ± 0.26	$(1.2 \pm 0.2) \times 10^{-4}$	3.3×10^{-6}

[a] The total pressure was 1.000 ± 0.002 Torr; the HOBr-treated ice-film thickness was 3.0 ± 0.2 μm at 191 K and 7.6 ± 0.2 μm at 210 K. [b] γ_t was calculated from eq 4 by using $N_L = 2$ at 3.0 ± 0.2 μm at 191 K and $N_L = 10$ at 7.6 ± 0.2 μm at 210 K using the data provided in ref 40. See text for details. [c] N_L was estimated to be 6 on the water-ice film.[41]

experiments where more data points were collected. A layered pore diffusion model was employed to correct for ice surface roughness, to obtain the "true" uptake coefficient γ_t. On the basis of previous studies, which were conducted under similar conditions,[39,40] H_2O ice films can be approximated as hexagonally close-packed spherical granules stacked in layers.[41] The true uptake coefficient, γ_t, is related to the value γ_w by

$$\gamma_t = \frac{\sqrt{3}\gamma_w}{\pi\{1 + \eta[2(N_L - 1) + (3/2)^{1/2}]\}} \quad (4)$$

where η is the effectiveness factor, and N_L is the number of granule layers.[41,42] Detailed calculations for these parameters can be found in refs 39 and 41. A tortuosity factor $\tau = 4$ and a true ice density $\rho_t = 0.925$ g/cm^3 were used in the above calculation.

Results

3.1. Uptake Coefficients for SO_2 on Ice Films with Various HOBr Coverages. Uptake of SO_2 on the Water-Ice Film. In this experiment, a 26-cm length of ice film was prepared on the wall of the flow reactor. Gaseous SO_2 was taken up by the water-ice film surface as monitored by the QMS at $m/e^- = 64$. The first-order loss rate k_s can be calculated using eq 1. The uptake coefficients γ_w of SO_2 on water-ice films were determined to be 4.4×10^{-5} at 190 K and 4.7×10^{-6} at 210 K. The detailed experimental conditions are included in Table 1.

Uptake Coefficient for SO_2 on HOBr-treated Ice Films. In this experiment, an ice film was vapor deposited on the wall of the flow reactor and HOBr was then exposed to the freshly prepared ice surface, as the sliding injector was slowly pulled out to cover the entire ice-film surface. The HOBr uptake amount (surface coverage) was determined by the QMS. Both HOBr exposure time (4−25 min) and partial HOBr pressure (typical $P_{HOBr} = 1.4 \times 10^{-6}$ Torr) were varied, to achieve different surface coverages. After the ice film had been treated with HOBr, SO_2, at a pressure of $(1.4 \pm 0.2) \times 10^{-6}$ Torr, was exposed to the HOBr-treated ice-film surface. The gas-phase loss of SO_2 was measured by the QMS as a function of the injector distance z. The pseudo-first-order rate constant, k_s, and the initial uptake coefficient, γ_w, for SO_2 on a HOBr-treated ice film were determined using eqs 1 and 3, respectively, and γ_w was measured as a function of the HOBr surface coverage (molecules/cm^2) at 191 K and at 210 K. The results are shown in Figure 3, and detailed experimental conditions are presented in Table 1. The errors listed in Table 1 and the error bars in Figure 3 include both 1 standard deviation $\pm\sigma$ of the mean value and systematic errors of the pressure gauges, digital thermometers, and mass flow meters, estimated to be approximately 8%. γ_t is corrected for porosity of the ice using eq 4 (see section 3.2). Figure 3 shows that the γ_w values increase from 9.3×10^{-5} to 1.4×10^{-3}, when the HOBr surface coverage increases from 8.2×10^{13} to 1.2×10^{15} molecules/cm^2, at 191 K. These values are higher than the γ_w of SO_2 on water-ice surfaces (which is shown in Figure 3 as well) at the same temperature. At 210 K, the initial uptake coefficient for SO_2, γ_w, increases from 7.8×10^{-6} to 1.2×10^{-4}, as the HOBr surface coverage increases from 3.1×10^{14} to 7.6×10^{14} molecules/cm^2. The initial uptake coefficients for SO_2 on the HOBr-treated ice film at 210 K are lower than those at 191 K.

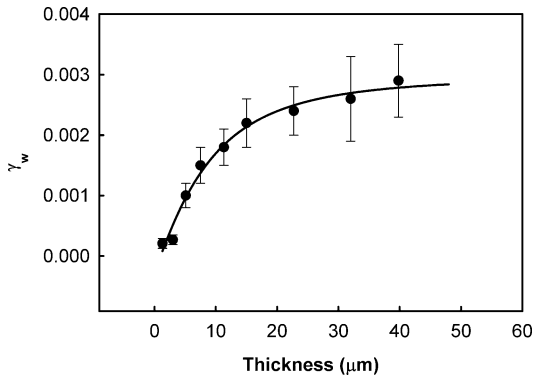

Figure 4. Plot of the initial uptake coefficient of SO_2, γ_w, on the HOBr-treated ice film is a function of the ice-film thickness at 191 K. The solid line is a nonlinear least-squares fit to the data using eq 4 and an empirical correlation $N_L = a + b \log(c + h)$, where parameters a, b, and c were fitted to be $a = -27.235$, $b = 24.858$, and $c = 11.329$ ($h = 1.3-40$ μm). See details in text. The plot shows that γ_w increases as the film thickness increases, and then the increase becomes gradual as the film gets thicker.

3.2. Effect of Ice-film Thickness on Initial Coefficients. In this experiment, we varied the ice-film thickness, h, at constant temperature and HOBr coverage. The initial uptake coefficient of SO_2 over the HOBr-treated ice film rapidly increases with the film thickness when h is less than 20 μm, and then γ_w increases gradually at $h > 30$ μm (Figure 4). This suggests that the HOBr-treated ice film is porous and has internal surface areas. SO_2 molecules can access internal surfaces by

TABLE 2: Uptake Coefficients of SO_2 on HOBr-treated Ice Surfaces at Varying Temperatures[a]

temperature (K)	P_{SO_2} (Torr)	v (m/s)	HOBr uptake amount (molecules/cm^2)	k_s (1/s)	k_w (1/s)	γ_w	γ_t[b]
190.0 ± 0.2	1.4×10^{-6}	2.0	3.4×10^{14}	33.5 ± 4.9	38.4 ± 5.7	$(2.6 \pm 0.4) \times 10^{-3}$	8.0×10^{-5}
195.0 ± 0.2	1.6×10^{-6}	2.0	3.7×10^{14}	16.5 ± 3.3	17.6 ± 3.6	$(1.2 \pm 0.2) \times 10^{-3}$	2.6×10^{-5}
200.2 ± 0.2	1.5×10^{-6}	2.1	3.4×10^{14}	6.38 ± 1.15	6.54 ± 1.19	$(4.3 \pm 0.8) \times 10^{-4}$	8.1×10^{-6}
205.0 ± 0.1	1.5×10^{-6}	2.1	3.1×10^{14}	1.51 ± 0.28	1.52 ± 0.29	$(9.9 \pm 1.9) \times 10^{-5}$	1.7×10^{-6}
209.9 ± 0.2	1.5×10^{-6}	2.3	3.8×10^{14}	0.63 ± 0.17	0.63 ± 0.17	$(4.1 \pm 1.1) \times 10^{-5}$	7.0×10^{-7}
214.9 ± 0.1	1.4×10^{-6}	2.3	7.0×10^{13}	0.24 ± 0.07	0.24 ± 0.07	$(1.5 \pm 0.4) \times 10^{-5}$	2.6×10^{-7}
219.9 ± 0.3	1.4×10^{-6}	2.3	5.1×10^{13}	0.23 ± 0.11	0.23 ± 0.11	$(1.5 \pm 0.7) \times 10^{-5}$	2.5×10^{-7}
229.6 ± 0.4	1.4×10^{-6}	2.4	4.3×10^{13}	0.25 ± 0.14	0.26 ± 0.14	$(1.6 \pm 0.8) \times 10^{-5}$	2.7×10^{-7}
240.6 ± 0.2	1.6×10^{-6}	2.6	1.8×10^{14}	0.59 ± 0.38	0.59 ± 0.38	$(3.6 \pm 2.3) \times 10^{-5}$	6.2×10^{-7}

[a] The total pressure was 2.000 ± 0.006 Torr; the H_2O−ice-film thickness was 32 ± 1 μm. [b] γ_t was calculated from eq 4 by using $N_L = 16$.[41] See text for details.

pore diffusion. However, at $h > 40$ μm, the pore diffusion time is probably comparable with the SO_2 surface residence time to prevent SO_2 molecules from effectively accessing all internal surfaces. The increase in γ_w is slow, and a plateau starts to appear in Figure 4. We modeled this behavior using the hexagonally close-packed spherical granules pore diffusion model.[41] Since N_L in eq 4 is a function of thickness, the solid line presented in Figure 4 was fitted to eq 4. The relationship between N_L and h was assumed to be $N_L = a + b \log(h + c)$, where parameters a, b, and c were determined from the nonlinear least-squares fit. On the basis of the fitted results, we determined $N_L \approx 2$ for a 3.0 μm HOBr-treated ice film at 191 K. This N_L value was used to calculate γ_t of 3 μm HOBr-treated ice films at 191 K, and the calculated γ_t values are presented in Table 1. The fitted N_L value is lower than the N_L value of water-ice at 3 μm reported by Keyser et al.[41] HOBr uptake on ice is an exothermal process. It is likely that the ice granule size is reconstructed after HOBr adsorbed on the ice granules. This changes the N_L-h distributions for a thin ice film. We expect that this process has less impact on a thicker film (>10 μm). Since a thicker film has more granule layers, the granule size reconstruction due to HOBr adsorption is anticipated at the top layers of the ice film; the number of granule layers N_L in a HOBr-treated ice film has remained approximately the same as the water-ice film.

3.3. Effect of Temperature on Initial Uptake Coefficient. In this experiment, we employed thicker ice films, 32 ± 1 μm and a higher total pressure in the flow reactor, 2.000 ± 0.006 Torr, to cover wider temperature ranges. The initial uptake coefficient of SO_2, γ_w, decreases from 2.6×10^{-3} to 1.5×10^{-5}, as the temperature of the HOBr-treated ice film increases from 190 to 215 K, while HOBr surface coverage is maintained approximately at $(3.4 \pm 0.4) \times 10^{14}$ molecules/cm^2. The partial pressure of HOBr is $(3.2 \pm 0.2) \times 10^{-6}$ Torr. On the basis of our previous study, HOBr starts to desorb from the water-ice surface at 215−225 K, which the precise value depends on the HOBr surface coverage.[35] The uptake amount of HOBr on water-ice is a function of the temperature. The amount of HOBr on the water-ice surface is maintained approximately at $(3.4 \pm 0.4) \times 10^{14}$ molecules/cm^2 when $T < 215$ K. Ice films are not able to take up as much HOBr when $T \geq 215$ K. Uptake decreases from 7.0×10^{13} to 4.3×10^{13} molecules/cm^2 as the temperature increases from 215 to 230 K, even at slightly higher $P_{HOBr} = (5.9 \pm 0.1) \times 10^{-6}$ Torr. The initial uptake coefficients of SO_2, within this temperature range, are nearly constant, 1.5×10^{-5}, within the uncertainty of the experiment. At 240 K, the initial uptake coefficient is slightly higher $(3.6 \pm 2.3) \times 10^{-5}$. Table 2 summarizes the results. γ_t is corrected for the ice-film porosity and assumes for simplicity that the SO_2 molecules are taken up by a geometrically smooth HOBr−ice surface. The profile for γ_t as a function of temperature is shown in Figure 5. The activation energy E_a of SO_2 on the HOBr-treated ice surface was calculated from the slope of the plot of log γ_t vs $1/T$ at 190−215 K. E_a was determined to be about −81 ± 8 kJ/mol (see details in section 4.2).

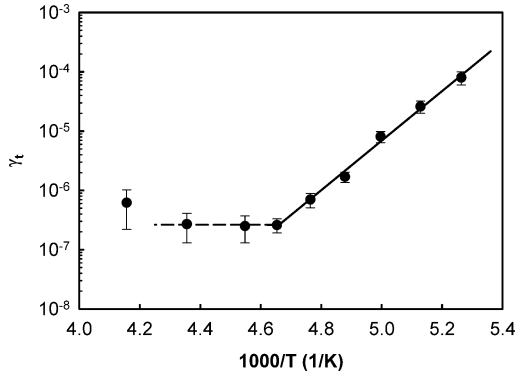

Figure 5. Plot of the logarithm of the "true" uptake coefficient of SO_2, γ_t, on the HOBr-treated ice surface vs $1/T$. The solid line was fitted to the experimental data at 190−215 K using the Arrhenius equation. The activation energy E_a was determined to be about −81 ± 8 kJ/mol, $P_{SO_2} = (1.5 \pm 0.1) \times 10^{-6}$ Torr, and total pressure is 2.000 ± 0.006 Torr. The HOBr-treated ice-film thickness is 32 ± 1 μm.

IV. Discussion

4.1. Uptake Coefficients of SO_2 on HOBr−Ice Films. Our experimental results showed that true uptake coefficients for SO_2 on the water-ice surface are 2.0×10^{-6} at 191 K and 1.3×10^{-7} at 210 K. These values can be up to approximately 90-fold lower than the values for uptake by HOBr-treated ice film at the same temperatures (see Table 1). The nature of the SO_2 uptake by the water-ice films is different from that by the HOBr-treated ice films. At 191 K, SO_2 is likely to be weakly adsorbed near the water-ice surface. In contrast, SO_2 is anticipated to be oxidized on the HOBr-treated ice film, on the basis of the SO_2 oxidation in the aqueous phase and the SO_2−HOBr chemistry.[24,25]

SO_2 on the Water-Ice Film. The uptake coefficient for SO_2 on the water-ice film is lower at 210 K than that at 191 K. This may be explained in terms of the precursor mechanism given below, as we described in an earlier publication[22]

$$SO_2(g) \underset{k_{-1}}{\overset{k_1}{\rightleftharpoons}} SO_2\ (\text{precursor}) \xrightarrow{k_2} SO_2(\text{ad}) \qquad (5)$$

The uptake coefficient can be expressed as[22]

$$\gamma_t = \frac{4k_1k_2}{\omega(k_{-1} + k_2)} \qquad (6)$$

where ω is the mean molecular velocity of SO_2. At 210 K, the SO_2 desorption rate out of the precursor state is higher than that at 191 K, that is, k_{-1} is higher at 210 K, and thus, the uptake coefficient is lower, according to eq 6. Equation 6 also shows the temperature-dependent behavior of the SO_2 uptake coefficient for the water-ice surface; this behavior is independent of the partial pressure of SO_2.

SO_2 on HOBr-treated Ice Films. The initial uptake coefficients were measured as a function of the HOBr surface coverage, at 191 and 210 K (Figure 3). γ_w was corrected for the ice porosity, using eq 4. Since SO_2 uptake by water-ice film surfaces is very low, on the basis of this work and our previous work,[22] and since HOBr is taken up by the ice film (see Figure 1), the results may be treated using Eley−Rideal kinetics. This is illustrated below

$$\mathrm{HOBr(g)} \underset{k_{-3}}{\overset{k_3}{\rightleftharpoons}} \mathrm{HOBr(ad)} \tag{7}$$

$$\mathrm{SO_2(g) + HOBr(ad)} \underset{k_{-4}}{\overset{k_4}{\rightleftharpoons}} \mathrm{[HOBr\cdots SO_2(ad)]} \xrightarrow{k_5} \mathrm{product} \tag{8}$$

The observed gas-phase SO_2 loss rate can be written as

$$-\frac{\mathrm{d[SO_2}(g)]}{\mathrm{d}t} = \{k_4[\mathrm{SO_2(g)}]\theta_{\mathrm{HOBr}} - k_{-4}[\mathrm{HOBr\cdots SO_2(ad)}]\}\frac{S}{V} \tag{9}$$

where $[SO_2(g)]$ is the SO_2 concentration, θ_{HOBr} is the surface coverage of HOBr on the ice surface, and S/V is the surface-to-volume ratio. We apply the steady-state approximation to $[HOBr\cdots SO_2(ad)]$, that is, $d[HOBr\cdots SO_2(ad)]/dt = 0$ and then substitute the result into eq 9. We thus have

$$-\frac{\mathrm{d[SO_2}(g)]}{\mathrm{d}t} = \frac{k_4k_5S}{(k_{-4}+k_5)V}[\mathrm{SO_2(g)}]\theta_{\mathrm{HOBr}} \tag{10}$$

The uptake coefficient γ_t can be expressed as

$$\gamma_t = \frac{-\dfrac{\mathrm{d[SO_2(g)]}}{\mathrm{d}t}}{\dfrac{[\mathrm{SO_2(g)}]\omega S}{4V}} = \frac{4k_4k_5}{\omega(k_{-4}+k_5)}\theta_{\mathrm{HOBr}} \tag{11}$$

Equation 11 indicates that γ_t is proportional to the HOBr surface coverage. We can also express eq 11 as

$$\gamma_t = k_h\theta_{\mathrm{HOBr}} \tag{12}$$

where $k_h = 4k_4k_5/\omega(k_{-4} + k_5)$, an overall rate constant, is the combination of all rate constants and conversion factors. This explains the experimental data (Figure 3) well: as HOBr coverage increases, the initial uptake coefficient increases. Also, the experimental data, γ_t, were fitted to eq 12; the results are shown in Figure 6. The overall rate constant k_h was determined from the slope of the fit to be 1.5×10^{-19} and 6.4×10^{-21} molecules^{-1} cm^2, at 191 and 210 K, respectively. The fitted line represents the experimental results well, except at higher HOBr coverage. Among possible reasons for the deviation at high coverage is the fact that the model is simple and omits some factors. For instance, adsorbed HOBr may form "islands"

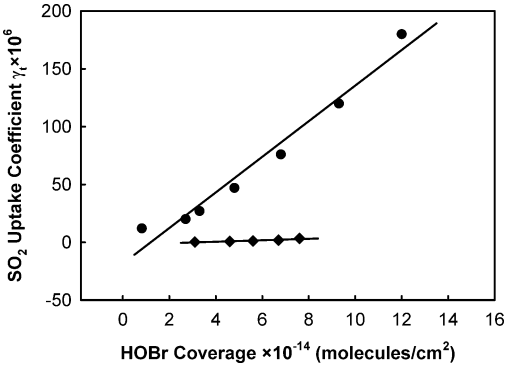

Figure 6. Plot of the SO_2 "true" uptake coefficient γ_t vs the HOBr surface coverage at 191 K (●) and 210 K (♦). Solid lines are fitted to eq 12, and the slope of the fit is k_h. The fitted lines suggest that the uptake of SO_2 on the HOBr-treated ice surface can be represented using the model outlined in the text.

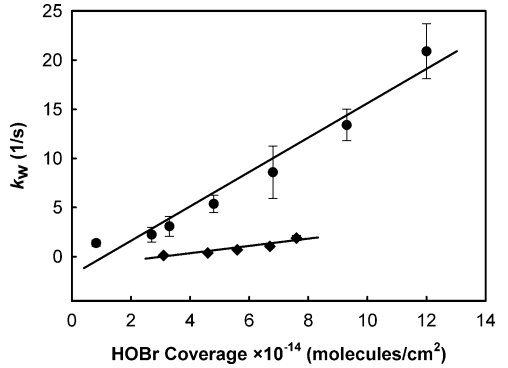

Figure 7. Plot of the pseudo-first-order rate constant k_w vs the HOBr surface coverage at 191 K (●) and 210 K (♦). The second-order rate constant was determined from the slope of the fit to be 1.8×10^{-14} molecules^{-1} cm^2 s^{-1} at 191, and 3.7×10^{-15} molecules^{-1} cm^2 s^{-1} at 210 K.

at higher coverage, on the ice surface.[35] Also, the uncertainty of measurement should be taken into consideration. The fitted parameter, k_h, should not be used to represent broad HOBr coverage ranges.

We can express the rate of the reaction in terms of

$$\mathrm{rate} = k_h^2\theta_{\mathrm{HOBr}}P_{\mathrm{SO_2}} \tag{13}$$

where k_h^2 is the second-order heterogeneous rate constant, which can be determined from a plot of k_w vs θ_{HOBr}. The plot is shown in Figure 7. k_h^2 was determined to be 1.8×10^{-14} and 3.7×10^{-15} molecules^{-1} cm^2 s^{-1}, at 191 and 210 K, respectively.

4.2. Uptake Coefficients at Varying Temperature. The uptake coefficient of SO_2 decreases as the temperature of the HOBr-treated ice film increases, from 190 to 215 K (Figure 5). The observation can be qualitatively explained by the above-described model (eq 11 or eq 12). The temperature dependence of the overall rate constant can be described using the Arrhenius equation. We have $\ln \gamma_t \propto -E_a/RT$. The activation energy was determined from a plot of $\log \gamma_t$ vs $1/T$ (as shown in Figure 5) for the temperature range of 191−215 K: $E_a = -81 \pm 8$ kJ/mol and $\gamma_t = 4.2 \times 10^{-27} \exp(9.77 \times 10^3/T)$. The negative E_a suggests that the transition-state complex $SO_2\cdots HOBr$ is stabilized by the ice surface. The desorption energy of HOBr on ice surfaces is approximately 67 ± 15 kJ/mol.[35] After the stabilization of the transition-state complex by the ice is taken into consideration, the value $E_a = -81 \pm 8$ kJ/mol is expected.

It is also expected that $\Delta S^{\ddagger}$ is negative as the transition state is adsorbed on the surface. At temperature >215 K, values for the uptake coefficient of SO_2 start to level off (see Figure 5), and they are maintained near a constant value in the temperature range of 215−230 K. This is likely due to desorption of HOBr from the ice film, and thus, k_{-4} increases (cf. eq 10). The net uptake of SO_2 by HOBr-treated ice is lower within this temperature range. The thermal energies of both SO_2 and HOBr molecules at $T > 230$ K are higher. The chances that the reaction overcomes its barrier are higher, and the value of the observed uptake coefficient starts to rise again.

We noted that the γ_w value at 190 K (32 μm, Table 2) is nearly 10-fold higher than that at 191 K and $\theta_{HOBr} = 3.4 \times 10^{14}$ molecules/cm^2 (3 μm, Table 1). We attribute this mainly due to the ice-film thickness. Figure 4 shows that γ_w increases approximately 14-fold as h increases from 1.3 to 40 μm. The ice-film porosity was corrected using the pore diffusion model. The corrected γ_t values are 5.1×10^{-5} (eq 12) and 8.0×10^{-5} (Table 2) at the HOBr coverage of 3.4×10^{14} molecules/cm^2 and 3 and 32 μm, respectively. Since the ice granule size is ~1 μm, we converted the ice-film thickness h into N_L for calculation purposes (see section 3.2). The correction is made at different N_L values, and it is discrete values. This introduces some uncertainty in γ_t. Also, other factors, such as ice-film preparation conditions, may also contribute to errors in initial uptake coefficient so that the agreement in γ_t at 3 and 32 μm is quite good as for a heterogeneous reaction on ice.

4.3. Comparison with Previous Studies. We can compare the measured uptake coefficient for SO_2 on water-ice films with previous reports.[22,23] Chu and co-workers reported a mean value of γ_t to be about 7×10^{-7} at 191.3 K.[22] Clegg and Abbatt studied the uptake of SO_2 on water-ice, but they did not provide an uptake coefficient value.[23] The present study found that γ_t is 2×10^{-6} at 190 K; this value is in reasonable agreement with our previous results,[22] after the small temperature difference and experimental uncertainty are taken into consideration.

There are no previously published data on the uptake coefficient for SO_2 on HOBr-treated ice surfaces. The uptake rate of SO_2 by HOBr-treated ice surfaces is comparable to that by H_2O_2−ice surfaces ($\gamma = 10^{-3}-10^{-4}$) at 191 K.[22] This suggests that uptake by HOBr−ice surfaces is a potentially pathway for SO_2 oxidation in the atmosphere. Oxidation of S(IV) by HOBr in solution has been studied, and the rate constants for the following reactions are

$$HOBr + SO_3^{2-} \xrightarrow{k_6} OH^- + BrSO_3^- \quad (14)$$

$$BrSO_3^- + H_2O \xrightarrow{k_7} Br^- + SO_4^{2-} + 2H^+ \quad (15)$$

$k_6 = 5 \times 10^9$ M^{-1} s^{-1} at 298 K and $k_7 = 230$ s^{-1} at 273 K.[24] Since there is an equilibrium between SO_2, HSO_3^-, and SO_3^{2-},[12] k_6 may be written in terms of P_{SO_2} and pH. Because rate constants in the aqueous phase are measured at very different conditions from the current study, we cannot make a direct quantitative comparison between them under the same experimental conditions.

We compare the relative rate of the SO_2 loss on the HOBr-treated ice surface to the oxidation rate over deliquescent sea-salt particles, assuming the values of aqueous-phase rate constants at lower temperature are similar to those at 298 K.[11] Using eqs 13 and 14 and typical atmospheric HOBr concentration, ~100 pptv, we can write the rates as

$$\text{rate}_{ice} = k_h^2 \theta_{HOBr} P_{SO_2} \approx 10 P_{SO_2} \quad (16)$$

and

$$\text{rate}_{solution} = k_6[HOBr][SO_3^{2-}] = k_6[HOBr]\frac{1.06 \times 10^{-9}}{[H^+]^2} P_{SO_2} \approx 50\, P_{SO_2} \quad (17)$$

where $\theta_{HOBr} \sim 5 \times 10^{14}$ molecules/cm^2, $[HOBr] = 100 K_H$, $K_H \sim 92$ M/atm is Henry law's constant,[11] $[SO_3^{2-}] = 1.06 \times 10^{-9} P_{SO_2}/[H^+]$,[2,13] and pH = 4.5. Equation 17 suggests that the rate of incorporation of SO_2 into solution and subsequent oxidation is comparable to the loss rate (oxidation) on the HOBr−ice surface (eq 16). The comparison assumes that the steady-state HOBr surface coverage remains unchanged near the ice surface at 191 K. Vogt and co-workers suggested that up to ~60% of S(IV) is oxidized by HOBr and HOCl in the MBL, on sea-salt ice aerosols.[11] S(IV) oxidation by HOBr on ice could constitute a pathway in the boundary layer, once a mechanism is established by which the supply of HOBr molecules to ice surfaces is maintained. This study suggests that heterogeneous SO_2 loss on the HOBr−ice surface is rather quick ($\gamma_w \sim 10^{-3}$) at 191 K provided there is sufficient HOBr coverage. When HOBr coverage is depleted, it changes the nature of the question. It becomes the loss of SO_2 on water-ice, where the uptake coefficient is low ($\gamma \sim 10^{-5}$)[22] and the reaction ceases. Also, at a warmer temperature >220 K, both the HOBr surface coverage and SO_2 uptake coefficient ($\gamma_w \sim 10^{-6}$) on the HOBr-treated ice decrease (see Table 2); the SO_2 oxidation on HOBr-treated ice surface is not an important process in the troposphere.

V. Conclusion

We have studied the uptake SO_2 on the HOBr-treated ice surfaces using a low-temperature flow reactor coupled with a differentially pumped quadrupole mass spectrometer. The initial uptake coefficient γ_w was determined as a function of HOBr coverage on ice-film surfaces. γ_w was determined to be in the range of 9.3×10^{-5} to 1.4×10^{-3} at 191 K and 7.8×10^{-6} to 1.2×10^{-4} at 210 K. The effect of temperature on the initial uptake coefficients was investigated, and the activation energy E_a was determined to be about -81 ± 8 kJ/mol at 190−215 K. The SO_2 uptake is discussed in terms of the Eley−Rideal mechanism. The present study suggests that uptake SO_2 by HOBr−ice surfaces is a rapid process provided HOBr coverage is maintained at 191 K, however, it is not a significant atmospheric pathway in the MBL where the temperature is higher than 220 K.

Acknowledgment. This work was supported by the National Science Foundation under Grant ATM-0355521.

References and Notes

(1) Barrie, L. A. *Atomos. Environ.* **1986**, *20*, 643.
(2) Koerner, R. M.; Fisher, D. *Nature* **1982**, *295*, 137.
(3) Finlayson-Pitts, B. J. *J. Geophys. Res.* **1993**, *98*, 14991.
(4) Mckeen, S. A.; Liu, S. C. *Geophys. Res. Lett.* **1993**, *20*, 2363.
(5) Barrie, L. A.; Hoff, R. M. *Atomos. Environ.* **1984**, *18*, 2711.
(6) Barrie, L. A.; Bottnheim, J. W.; Schnell, R. C.; Crutzen, P. J.; Rasmussen, R. A. *Nature* **1988**, *334*, 138.
(7) Impey, G. A.; Shepson, P. B.; Hastie, D. R.; Barrie, L. A.; Anlauf, K. G. *J. Geophys. Res.* **1997**, *102*, 16005.
(8) Fan, S. M.; Jacob, D. J. *Nature* **1992**, *359*, 522.

(9) Colin, J. L.; Renard, D.; Lescoat, V.; Jaffrezo, J. L.; Gros, J. M.; Strauss, B. *Atmos. Environ.* **1989**, *23*, 1487.
(10) Tranter, M.; Brimblecombe, P.; Davies, T. D.; Vincent, C. E.; Abvehams, P. W.; Blackwood, I. *Atmos. Environ.* **1986**, *20*, 517.
(11) Vogt, R.; Crutzen, P. J.; Sander, R. *Nature* **1996**, *383*, 327.
(12) Krischke, U.; Staubes, R.; Brauers, T.; Gautrois, M.; Burkert, J.; Stöbener, D.; Jaeschke, W. *J. Geophys. Res.* **2000**, *105*, 14413.
(13) Seinfeld, J. H.; Pandis, S. N. *Atmospheric Chemistry and Physics*; Wiley: New York, 1998; Chapters 6 and 19.
(14) Valdez, M. P.; Bales, R. C.; Stanley, D. A.; Dawson, G. A. *J. Geophys. Res.* **1987**, *92*, 9779.
(15) Hoppel, W.; Pasternack, L.; Caffrey, P.; Frick, G.; Fitzerald, J.; Hegg, D.; Gao, S.; Ambrusko, J.; Albrechcinski, T. *J. Geophys. Res.* **2001**, *106*, 27575.
(16) Choi, J.; Conklin, M. H.; Bales, R. C.; Sommerfeld, R. A. *Atmos. Environ.* **2000**, *34*, 793.
(17) Diehl, K.; Mitra, S. K.; Pruppacher, H. R. *Atmos. Res*. **1998**, *47*−*48*, 235.
(18) Mitra, S. K.; Barth, S.; Pruppacher, H. R. *Atmos. Environ*., *Part A* **1990**, *24*, 2307.
(19) Sommerfeld, R. A.; Lamb, D. *Geophys. Res. Lett.* **1986**, *13*, 349.
(20) Conklin, M. H.; Sommerfeld, R. A.; Laird, S. K.; Villinski, J. E. *Atmos. Environ., Part A* **1993**, *27*, 159.
(21) Conklin, M. H.; Bales, R. C. *J. Geophys. Res.* **1993**, *98*, 16851.
(22) Chu, L.; Diao, G. W.; Chu, L. T. *J. Phys. Chem. A* **2000**, *104*, 7565.
(23) Clegg, S. M.; Abbatt, J. P. D. *Atmos. Chem. Phys.* **2001**, *1*, 73.
(24) Troy, R. C.; Margerum, D. W. *Inorg. Chem.* **1991**, *30*, 3538.
(25) Hartz, K. E. H.; Nicoson, J. S.; Wang, L.; Margerum, D. W. *Inorg. Chem.* **2003**, *42*, 78.
(26) Keene, W. C.; Sander, R.; Pszenny, A. A. P.; Vogt, R.; Crutzen, P. J.; Galloway, J. N. *J. Aerosol Sci.* **1998**, *29*, 339.
(27) Impey, G. A.; Mihele, C. M.; Anlauf, K. G.; Barrie, L. A.; Shepson, P. B. *J. Atmos. Chem.* **1999**, *34*, 21.
(28) Chu, L. T.; Heron, J. W. *Geophys. Res. Lett*. **1995**, *22*, 3211.
(29) Chu, L. T. *J. Vac. Sci. Technol., A* **1997**, *15*, 201.
(30) Chu, L.; Chu, L. T. *J. Phys. Chem. A* **1999**, *103*, 691.
(31) Keyser, L. F.; Leu, M.-T. *J. Colloid Interface Sci.* **1993**, *155*, 137.
(32) Haynes, D. R.; Tro, N. J.; George, S. M. *J. Phys. Chem*. **1992**, *96*, 8502.
(33) Toth, Z.; Fabian, I. *Inorg. Chem.* **2004**, *43*, 2717.
(34) Fickert, S.; Adams, J. W.; Crowley, J. N. *J. Geophys. Res.* **1999**, *104*, 23719.
(35) Chu, L.; Chu, L. T. *J. Phys. Chem. A* **1999**, *103*, 8640.
(36) Brown, R. L. *J. Res. Natl. Bur. Stand. (U.S.)* **1978**, *83*, 1.
(37) Cussler, E. L. *Diffusion, mass transfer in fluid systems*; Cambridge University Press: New York, 1984; Chapter 4.
(38) Chu, L. T.; Leu, M.-T.; Keyser, L. F. *J. Phys. Chem.* **1993**, *97*, 12798.
(39) Keyser, L. F.; Moore, S. B.; Leu, M.-T. *J. Phys. Chem.* **1991**, *95*, 5496.
(40) Keyser, L. F.; Leu, M.-T. *Microsc. Res. Tech.* **1993**, *25*, 343.
(41) Keyser, L. F.; Leu, M.-T.; Moore, S. B. *J. Phys. Chem.* **1993**, *97*, 2800.
(42) Chu, L. T.; Leu, M.-T.; Keyser, L. F. *J. Phys. Chem.* **1993**, *97*, 7779.